Synthesis and electrochemical study of a hybrid structure based on PDMS-TEOS and titania nanotubes for biomedical applications

2014 Nanotechnology 25 365701

(http://iopscience.iop.org/0957-4484/25/36/365701)

IOP Publishing Nanotechnology
Nanotechnology **25** (2014) 365701 (10pp) doi:10.1088/0957-4484/25/36/365701

Synthesis and electrochemical study of a hybrid structure based on PDMS-TEOS and titania nanotubes for biomedical applications

António G B Castro[1,3], Alexandre C Bastos[1], Vardan Galstyan[2], Guido Faglia[2], Giorgio Sberveglieri[2] and Isabel M Miranda Salvado[1]

[1] Department of Materials and Ceramic Engineering/CICECO, University of Aveiro, Campus Universitário de Santiago, 3810-193 Aveiro, Portugal
[2] Sensor Lab, Department of Information Engineering, University of Brescia and CNR INO, Via Valotti 9, I-25133 Brescia, Italy

E-mail: acbastos@ua.pt

Received 16 May 2014
Accepted for publication 15 July 2014
Published 20 August 2014

Abstract

Metallic implants and devices are widely used in the orthopedic and orthodontic clinical areas. However, several problems regarding their adhesion with the living tissues and inflammatory responses due to the release of metallic ions to the medium have been reported. The modification of the metallic surfaces and the use of biocompatible protective coatings are two approaches to solve such issues. In this study, in order to improve the adhesion properties and to increase the corrosion resistance of metallic Ti substrates we have obtained a hybrid structure based on TiO_2 nanotubular arrays and PDMS-TEOS films. TiO_2 nanotubes have been prepared with two different diameters by means of electrochemical anodization. PDMS-TEOS films have been prepared by the sol–gel method. The morphological and the elemental analysis of the structures have been investigated by scanning electron microscopy and energy dispersive spectroscopy (EDS). Electrochemical impedance spectroscopy (EIS) and polarization curves have been performed during immersion of the samples in Kokubo's simulated body fluid (SBF) at 37 °C to study the effect of structure layers and tube diameter on the protective properties. The obtained results show that the modification of the surface structure of TiO_2 and the application of PDMS-TEOS film is a promising strategy for the development of implant materials.

Keywords: sol–gel coatings, TiO_2 nanotubes, electrochemistry, biomedical applications

(Some figures may appear in colour only in the online journal)

1. Introduction

Metallic orthopedic devices and implants are currently one of the main therapeutic solutions for bone and dental injuries. The critical factors determining the application of a material for biomedical implants are its biocompatibility followed by corrosion resistance. Besides, prosthesis failures can occur due to the weak bonding between the bone and the metal surface, and differences in their mechanical properties.

Titanium is one of the most employed materials in the production of implants and orthopedic devices. However, problems concerning localized corrosion and release of metallic ions have been reported [1–3]. Passivation of the titanium surface has been carried out by means of anodic or thermal oxidation [4, 5]. Thickness of oxide formed on the titanium is not affected by the grain size of the titanium substrate [6]. However the same results showed that the

[3] Current address: Department of Biomaterials, Radboud University Medical Center, Philips van Leydenlaan 25, 6525 EX Nijmegen, The Netherlands.

corrosion resistance of titanium substrate with the nanometric grain size is lower in comparison with the microgranular substrate [6]. On the other hand, bioactivity is enhanced by a nanostructured titania surface in comparison with the micro-textured titanium surface, as observed by Zhao *et al* [7].

The morphology of oxidized titanium is possible to modify during the anodic oxidation process in fluoride containing electrolytes [8]. TiO_2 nanostructures with the porous and tubular shapes are formed by adjustment of anodization parameters [9–12]. Such structures have been applied successfully in fabrication of excitonic solar cells, photocatalyst materials, chemical gas sensors and Li-ion micro batteries due to their high specific surface area and unique physical-chemical properties [12–18]. Oxidation of titanium and the formation of tubular TiO_2 layers increase the corrosion resistance and promote better adhesion of the prosthesis to the surrounding tissues and a greater interlocking of the cells [4, 19, 20]. Therefore the improvement of corrosion properties and the enhancement of bioactivity of TiO_2 nanotubes are very actual topics.

The application of different coatings enhances not only the corrosion resistance of the metallic substrates but also is known to promote a better adhesion between the metallic prosthesis and the tissue and therefore the biocompatibility [1, 21–24].

Ormosils (organic modified silicates) are silicon organic-inorganic hybrids that are commonly prepared by sol–gel methods. Recent investigations have shown that they have great potential as thin-film layer coatings for application in metallic prosthesis and other clinical devices. Such coatings showed high biocompatibility, good mechanical properties and a great linkage strength between the metallic surface and the SiO_2 units of the sol–gel [2, 25–27]. The sol–gel method has some advantages when compared with other techniques: it is a low-cost procedure, uses mild temperatures, allows the coating of complex geometries, the majority of the reagents are non-toxic and by tuning the experimental conditions different functional materials can be obtained [3, 28].

Gallardo *et al* [1] used a tetraethylorthosilicate (TEOS) and methyltriethoxisilane (MTES) hybrid sol–gel coating in stainless steel surfaces (AISI 316L), observing the formation of crack-free coatings and an improvement in the corrosion resistance of the metallic substrates. An improvement in the corrosion resistance of AISI 316L substrates was also observed by Hosseinalipour *et al* when a TEOS and 3-methacryloxypropyltrimethoxysilane (TMSM), in presence of benzoyl peroxide (BPO) as initiator agent, sol–gel hybrid was applied [3]. An improvement in the cell's adhesion was also observed, which is related with an increase in the surface's hydrophilicity.

Polydimethilsiloxane (PDMS) and TEOS hybrids are widely used in the preparation of biocompatible sol–gel substrates. This polymer is highly biocompatible, demonstrating high flexibility and thermal/oxidative stability [2, 25, 29, 30]. Also, coatings based on PDMS and inorganic SiO_2 (including TEOS precursor) have shown the formation of homogeneous crack-free surfaces, suitable for the production of potential anticorrosive coatings [2, 25, 29, 31].

In this work we report the development of a novel hybrid structure based on organic-inorganic PDMS-TEOS sol–gel film and TiO_2 nanotubes with improved topography and increased anticorrosive properties, suitable for clinical applications. The preparation and electrochemical characterization of the hybrid structure is reported together with the influence of the structure components on its protective properties.

2. Materials and methods

2.1. Fabrication of titania nanotubes

Titania nanotube arrays were fabricated by electrochemical anodization. Prior to anodization, titanium discs (0.5 mm thick, 9 mm diameter) were cleaned with acetone, ethanol and distilled water in ultrasonic bath. The anodization process was performed in two-electrode electrochemical cell with a Pt foil as cathode and the titanium discs as anodes. The electrolyte was 10 M H_2O and 0.5 wt% NH_4F glycerol solution. Anodization was carried out at potentials between 25 and 100 V for 90 min at room temperature, using a power supply (Delta Elektronika SM 300-5) connected to a PC for data acquisition and control. The average anodization current density was calculated and registered for every three seconds of the process. Crystallization of as-prepared structures from amorphous to anatase phase was carried out by thermal annealing according to a previous report [18].

2.2. Coating preparation

The reagents used to synthesize the hybrid coatings were: tetraethyl orthosilicate (TEOS), isopropanol, polydimethylsiloxane (PDMS) silanol terminated (550 g mol^{-1} average molecular weight), titanium isopropoxide (TiPr) and hydrochloric acid (HCl), all from Sigma-Aldrich, and ethyl acetoacetate (EtAcAc) from Merck.

Coatings were prepared with the following fixed molar ratios: TEOS:PDMS = 1.5, TEOS:TiPr = 6, TEOS:H_2O = 0.3 and TEOS:HCl = 22.2.

TEOS and PDMS were dissolved in isopropanol medium (half of the volume) and H_2O and HCl were added posteriorly, in order to promote the hydrolysis of the precursors followed by their condensation. After 2 h of stirring, a second solution using the other half of isopropanol amount and TiPr, previously chelated with ethyl acetoacetate, was added. The final mixture was then stirred for another 3 h at room temperature.

The coating was applied by a dip coating process as follows: samples were dipped at a 10 cm min^{-1} rate in the sol–gel solution, left immersed for 2 min and then withdrawn at the same rate. After the coating procedure the samples were aged for 24 h at room temperature and then gently heated in a two-step process in order to obtain homogenous coatings: they were placed first in an oven at 60 °C during 48 h for the coating to gellify, and finally dried at 150 °C for 24 h.

A schematic of the obtained hybrid structure is shown in figure 1. To investigate the influence of the different layers on

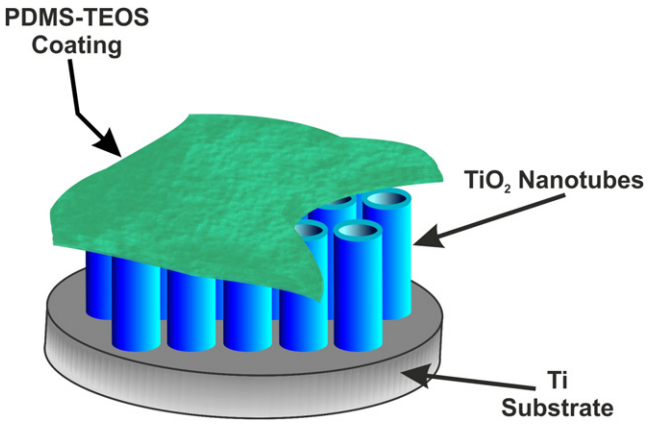

Figure 1. Schematic representation of the hybrid structure: Ti metallic substrate, TiO_2 nanotube arrays and PDMS-TEOS sol–gel coating.

Table 1. Investigated structures.

Sample	Nanotubes diameter (nm)	PDMS-TEOS sol–gel coating
Ti	—	—
Ti-TNT65	65	—
Ti-TNT135	135	—
Ti-SG	—	+
Ti-TNT65-SG	65	+
Ti-TNT135-SG	135	+

the properties of the hybrid structure, different samples were produced and tested, as given in table 1, where Ti refers to metallic titanium, Ti-TNT means Ti with TiO_2 nanotubes and SG denotes sol–gel film.

2.3. Sample characterization

Structural and elemental analysis were carried out by scanning electron microscopy (SEM, Hitachi SU-70 and LEO 1525 microscopes) and EDS (Rontec) with an accelerating voltage of 25 kV.

Electrochemical studies were performed with an AUTOLAB PGSTAT 302N potentiostat in a three electrode arrangement with a saturated calomel electrode (SCE) as reference (with a Luggin–Haber capillary), a coiled platinum wire as counter electrode and the samples as working electrode. The back of each sample was electrically connected to a copper cable with conductive glue and isolated with beeswax except for the testing surface. The testing solution was SBF [32] at about 37 °C. During the measurements the electrochemical cell was inside a Faraday cage.

Anodic and cathodic polarization curves were obtained by scanning from the open circuit potential (OCP) up to +3.0 V (anodic curve) or down to −2.0 V (cathodic curve) at a scan rate of 1 mV s^{-1}.

EIS experiments were performed applying an amplitude of 10 mV rms around OCP, with frequencies ranging from 100 kHz to 10 mHz and with seven points per decade logarithmically distributed.

Numerical fitting of the EIS results was performed using ZView (Scribner Associates USA) software.

3. Results and discussion

3.1. Formation of the TiO_2 nanotubes

TiO_2 nanotubes with two different diameters were fabricated. Morphological investigations show that the structure of TiO_2 arrays strongly depends on applied voltage. Highly-ordered and smooth-walled TiO_2 nanotubes are obtained at 25 and 50 V with the average inner diameters 65 and 135 nm, respectively (figures 2(a) and (c)). The distribution of the nanotubes over the substrates is very homogenous.

As can be seen in figure 2(d) the anodization current density decreases sharply during the first minutes of the process at both applied potentials due to the oxide layer formation on the surface of titanium. Consequently slight decrease of current density is due to the solubility of the formed barrier oxide layer and the formation of nanopores in fluoride containing electrolytes [8, 33]. The TiO_2 nanotubes are formed and the current reaches the steady stage, as the result of the equilibrium between the oxidation and the field-enhanced dissolution of the TiO_2.

3.2. Sol–gel film characterization

As can be seen in figure 3 the sol–gel film for the Ti-TNT65-SG samples presents thicker and more homogeneous coating (figures 3(a) and (b)) compared with the Ti-TNT135-SG samples (figures 3(c) and (d)). The difference in thickness between these two substrates is probably due to the penetration of the sol–gel solution in the nanotubes with larger diameter (135 nm), during the aging and drying steps, enabling the visualization of the nanotubes with higher magnification. EDS result enabled to identify elements such as titanium (Ti), silicon (Si), carbon (C) and oxygen (O), confirming the covering of the substrates with the PDMS-TEOS sol–gel solution.

3.3. Electrochemical measurements

Figure 4 shows the cathodic polarization curves of the different samples with one hour of immersion in SBF at 37 °C. The Ti-TNT65 and Ti-TNT135 surfaces showed the highest currents (starting from 10^{-6}–10^{-5} A cm^{-2}). The remaining curves started with very small currents (3–4 orders of magnitude lower than the samples with nanotubes) that increased as the potential became more negative. The smallest currents appeared on Ti-SG and Ti-TNT65-SG. All cathodic polarization curves depict the reduction of dissolved oxygen and, at more negative potentials, the reduction of water with hydrogen evolution. The approximate region where each reaction dominates is presented in figure 5. The reduction of dissolved oxygen dominates from OCP until the points signed as B (blue arrows), being controlled by activation from OCP

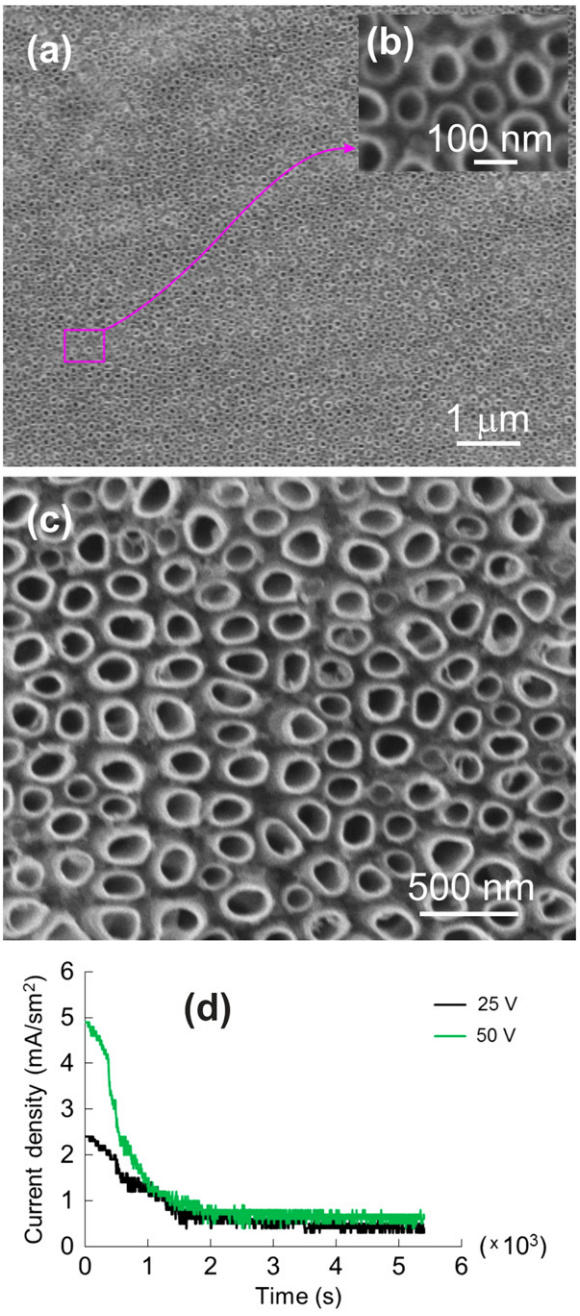

Figure 2. (a) SEM image of the nanotube arrays obtained at 25 V for 90 min. (b) Magnification of (a). (c) SEM image of the sample anodized at 50 V. (d) Dependence of anodization current density versus time for the samples anodized at 25 and 50 V.

to A (red arrows) and by diffusion from A to B. Then, for more negative potentials, oxygen still reacts but the measured current becomes dominated by the current of reduction of water with hydrogen evolution.

The shapes of all curves denote the influence of ohmic drop, particularly for those coated with sol–gel film. This ohmic drop comes not from the uncompensated solution resistance, which was small due to the placement of the reference electrode close to the working electrode by means of a Luggin–Haber capillary (that also prevented the leakage of Cl^- from the reference electrode into the SBF solution) but from the high resistance imposed by the surface oxide film and the SG film. The sol–gel coated samples presented the lowest currents but the cathodic processes were able to proceed despite the presence of the films. The higher currents for the surfaces with nanotubes can be an indication of the faster intrinsic kinetics of those reactions on such surfaces but may also be simply a reflection of the larger effective area due to their nanostructured surface.

Figure 6 presents the effect of cathodic polarization in the adhesion and stability of the sol–gel films. The sweep in the cathodic direction shows small values for the oxygen reduction while, when cycling back, the currents for the same reaction are much higher. It is likely that the high pH induced by the polarization affects the interfacial region, destroying the adhesion or even the integrity of the film, thus increasing the electroactive area and consequently the current. This result shows the importance of starting the cathodic measurement from OCP and not from the highest negative value, as commonly found in polarization curves when both cathodic and anodic branches are obtained in a single scan. It must be referred that the potential values applied in these experiments are much higher than the ones presented in biological environments, and so in such conditions this coating disruption phenomenon is highly improbable to occur.

The anodic polarizations curves measured after 1 h of immersion are depicted in figure 7. Three main regions can be recognized: from OCP to ~1.25 V, there is a region of small current with little variation: 10^{-9}–10^{-8} A cm^{-2} on the sol–gel coated samples, 10^{-8}–10^{-7} A cm^{-2} on the Ti-TNT substrates and higher values, up to 10^{-5} A cm^{-2}, on Ti. Then, a significant rise in current occurs until ~2 V. Finally, from 2 to 3 V, a new increase in current is observed in all samples except for the Ti-TNT-SGs.

The first region of the anodic curves, from OCP to ~1.25 V, shows passive currents that can be grouped and ranked, from the low current and more corrosion resistant sol–gel coated samples, to the surfaces with nanotubes and then to bare Ti. For the interpretation of the remaining regions, the work of Mazzarolo *et al* [34] is taken as reference. After ~1.25 V and up to ~2 V all samples showed a significant increase in current which is interpreted as a growth of the oxide layer, driven by the applied potential with migration of Ti^{4+} and O^{2-} in opposite directions. For higher potentials no further increase in oxidation of Ti takes place and the additional increase in current that is measured is due to the oxidation of water with evolution of O_2. On the samples with TNT+SG, no appreciable increase in current was observed for potentials higher than +2 V (and up to the highest tested potential, +3 V) what could be an indication of the high barrier of the sol–gel film that prevented the contact of water with the electrode surface. However, as discussed in the analysis of the cathodic polarization curves, the solution indeed seems to reach the electroactive surface. Thus, the absence of current increase may be due to the initial formation of O_2 bubbles that block the pathways in the sol–gel film, preventing its release from the surface and further ingress of solution.

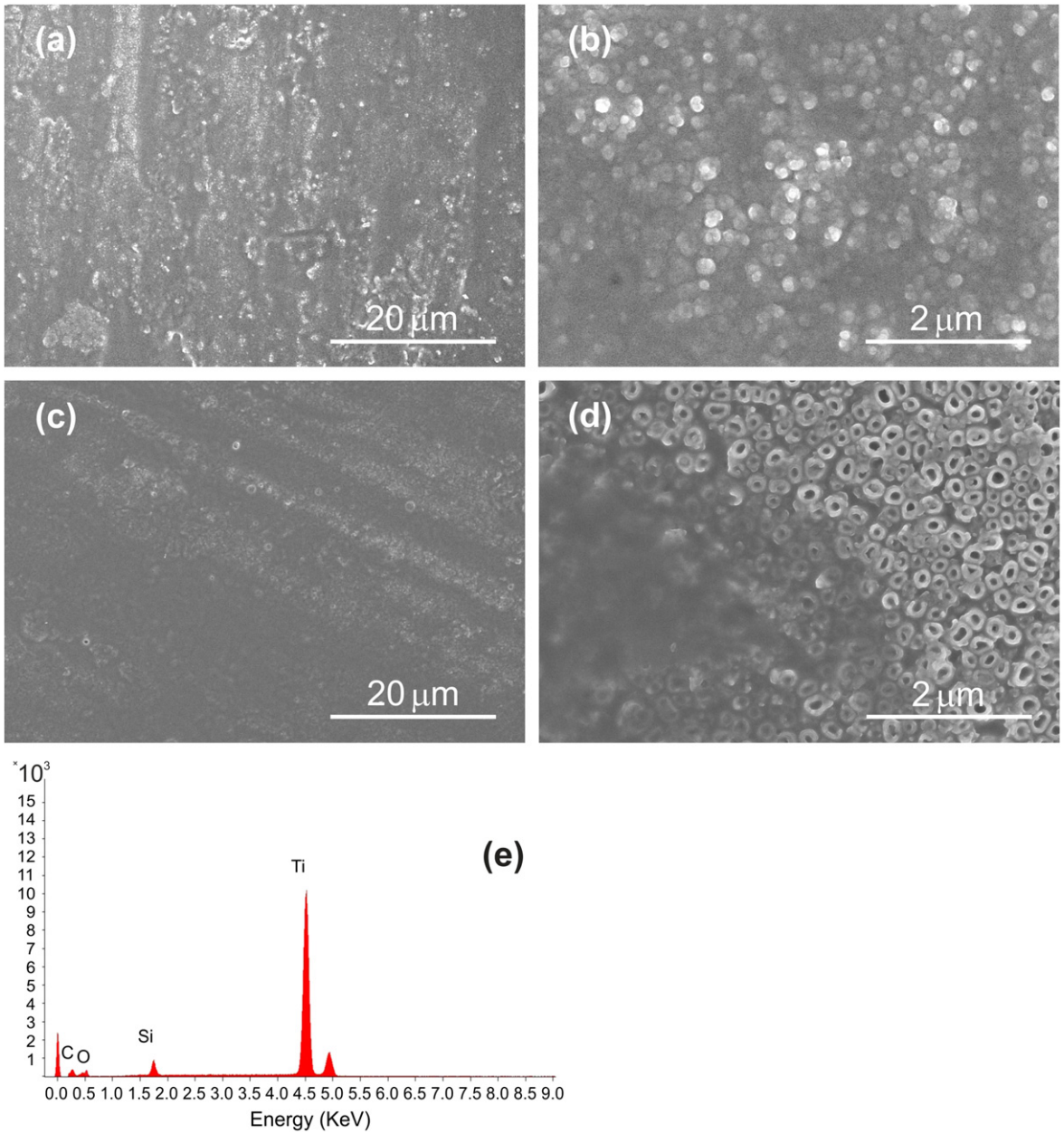

Figure 3. SEM images of sol–gel coated samples: Ti-TNT65-SG (a) and (b) Ti-TNT135-SG (c) and (d). (e) EDS result of the Ti-TNT65-SG sample.

The polarization curves show that the sol–gel has a passivating effect on the Ti oxidation and prevents the oxygen evolution, while the TiO_2 nanotubes have a passivating effect on the Ti oxidation but lead to the same oxygen evolution found in Ti. The anodic scan up to +3 V does not destroy the sol–gel film protection, contrarily to what was found with the cathodic polarization.

Figure 8 presents the impedance response for the different samples after immersion for 1 h, 1 day and 3 weeks. As can be observed in the Bode spectra (log of impedance modulus versus log frequency) all samples present high impedance (10^6–$10^8\ \Omega\,cm^{-2}$), being the highest impedance, corresponding to the highest corrosion resistance, found on the sol–gel coated samples, with the order being NT65-SG > Ti-SG > NT135-SG. As the immersion time increases the impedance diminishes, especially for samples Ti-TNT65-SG and Ti-TNT135-SG. The impedance of the samples without sol–gel followed the order Ti > Ti-TNT65 > Ti-TNT135 and identical behavior was observed: a resistive response at high frequencies (curve parallel to the *x*-axis) and a capacitive response on the remaining frequency range. The impedance was lower compared to the coated samples but still high, typical of passive surfaces. Just small variations were detected during the three weeks of testing. EIS analysis puts in evidence the good resistance to corrosion of the studied systems, with all showing high impedance and capacitive behavior.

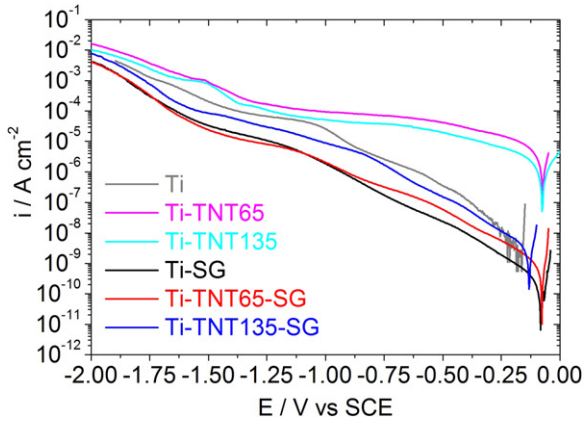

Figure 4. Cathodic polarization curves after 1 h of immersion in SBF at 37 °C.

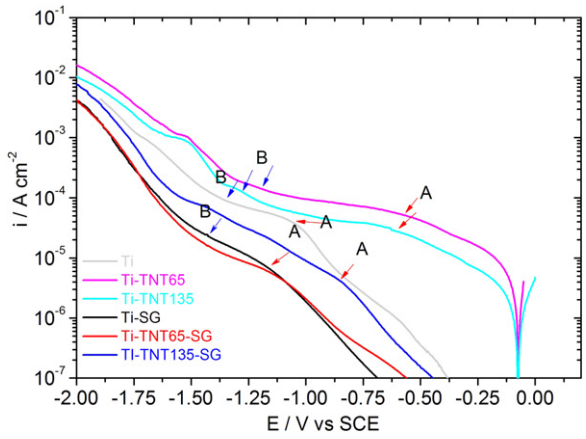

Figure 5. Approximate domains of each cathodic reaction: activation control of the reduction of dissolved O_2 from OCP to A, diffusion control from A to B and from B to more negative potentials reduction of water with hydrogen evolution.

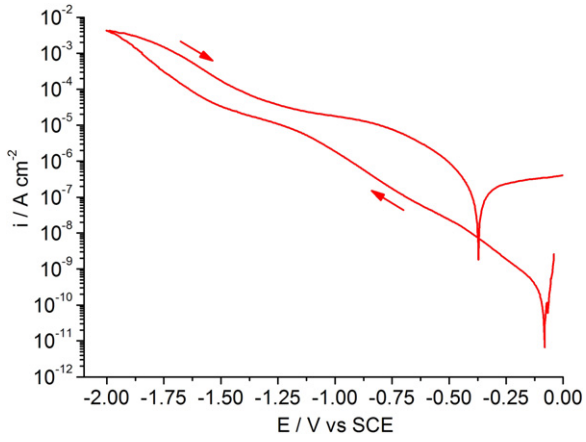

Figure 6. Cathodic polarization curves for a sol–gel coated sample after 1 h of immersion.

It is possible to obtain quantitative parameters from the impedance results. A typical approach is to fit the experimental data with equivalent electric circuits that can be regarded as analogues of the physico-chemical systems under study. Various circuits have been proposed in the literature for the systems under analysis and the most pertinent ones are presented in figure 9.

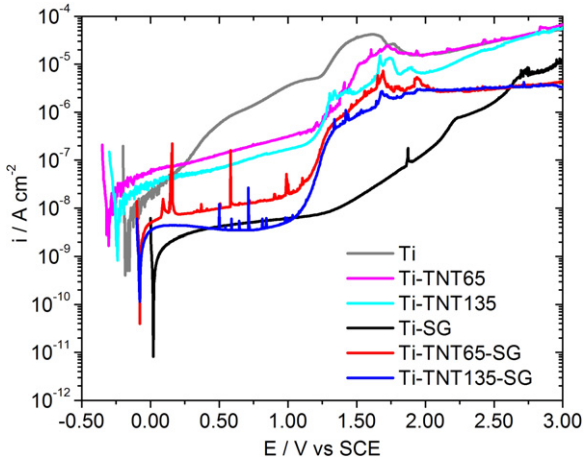

Figure 7. Anodic polarization curves after 1 h of immersion in SBF at 37 °C.

For Ti a circuit consisting of R_u (uncompensated resistance between working and reference electrodes) in series with a network with a resistance and a capacitance in parallel was used—figure 9(a). R_{surf} and C_{surf} are generic terms for surface resistance and surface capacitance. Usually R and C are the charge transfer resistance (R_{ct}) and the double layer capacitance (C_{dl}) [35] or oxide resistance (R_{ox}) and oxide capacitance (C_{ox}) [35–37]. Sometimes two parallel RC networks, ($R_{ct}C_{dl}$) and ($R_{ox}C_{ox}$), are placed in series to account for the effect of both oxide and electrochemical processes. It must be stressed that, as pointed out by Contu *et al* [38], when two capacitances are in series, it is likely that only the response of a single equivalent capacitance is measured. The same applies to resistances in series. In such cases, the resulting equivalent circuit becomes similar to 9(a) and generic terms like C_{surf} and R_{surf} are preferred.

TiO_2 nanotubes are considered to have a two layer structure: a barrier (or inner) layer and a porous (or outer) layer. A circuit with two parallel RC networks, one for each layer, placed in series has been employed by several authors [4, 39, 40]. The same circuit elements can be distributed in a different way resulting in a circuit that is frequently used [37, 41–44] and also adopted here. This circuit is shown in figure 9(b) where the subscripts PL and BL stand for porous layer and barrier layer, respectively.

When a sol–gel film is present, an extra RC network with sol–gel film resistance (R_{SG}) and sol–gel capacitance (C_{SG}) is added to the previous circuits. For Ti-SG, circuit 9(b) was used with the subscripts PL and BL being replaced, respectively, by SG and surf. Circuit 9(c) is proposed for TNT-SG. In these circuits the impedance response is dominated by the smallest capacitance and the remaining circuit only responds when defects or pores are present. R_{SG} is the resistance of the solution inside pores and defects of the sol–gel film.

Figure 10 shows the results of the numerical fitting replacing capacitors with constant phase elements (CPE),

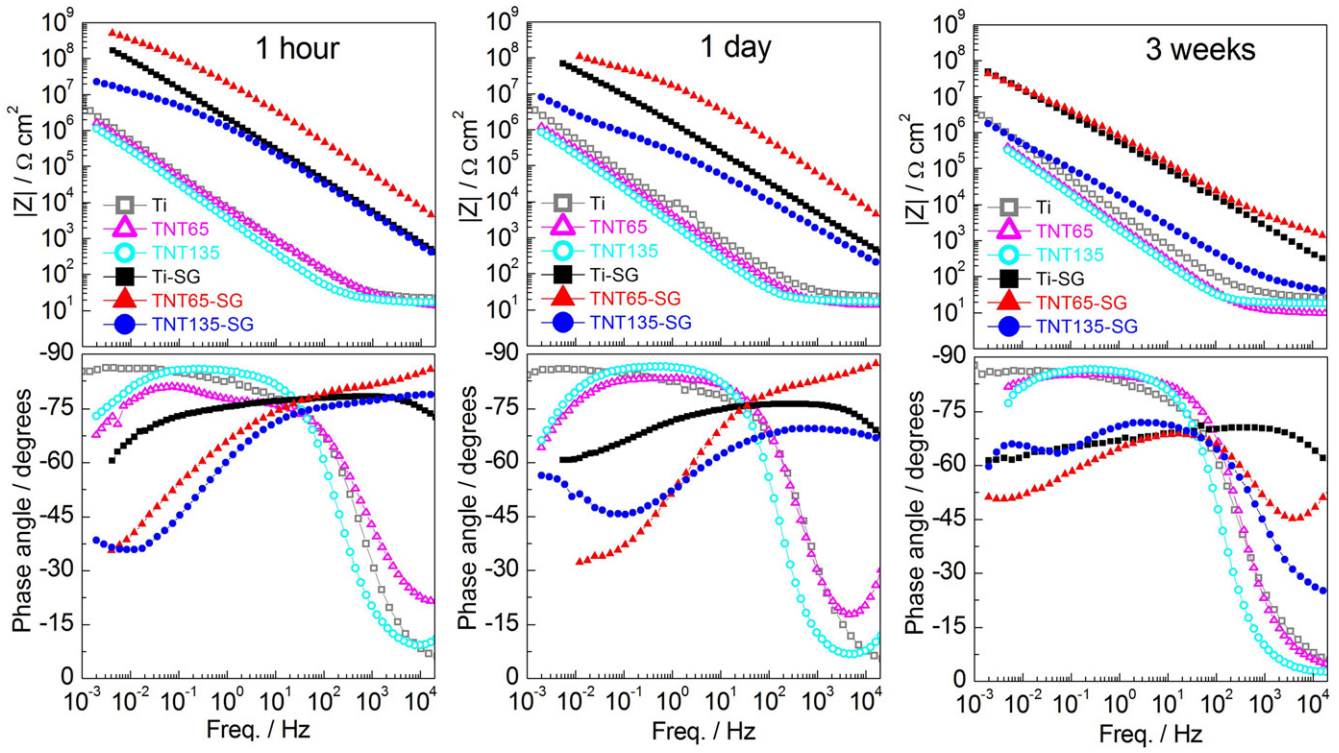

Figure 8. Bode plots for uncoated and coated substrates at different immersion times: 1 h, 1 day and 3 weeks.

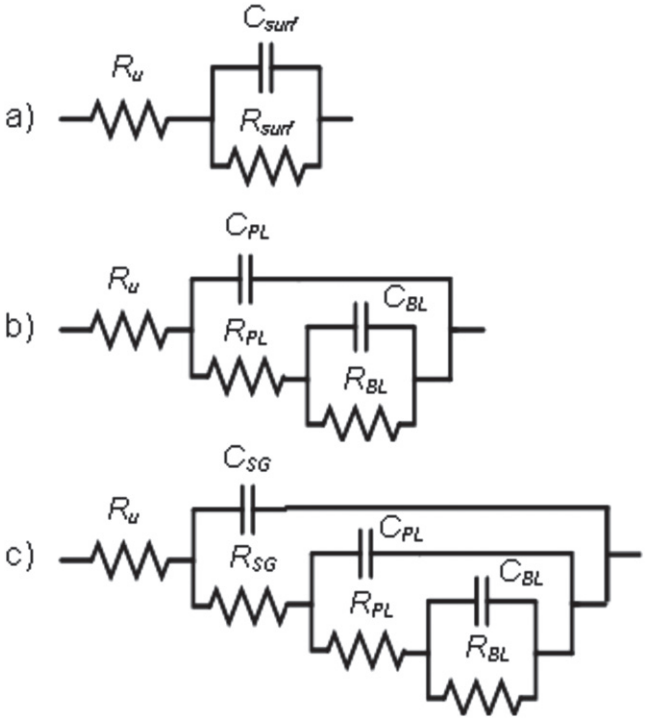

Figure 9. Equivalent electric circuits as analogues of the studied systems.

whose impedance is given by

$$\mathrm{ZCPE} = Y_0^{-1}(j\omega)^{-n}, \qquad (1)$$

where Y_0 is the frequency independent admittance, n is the power of CPE, $j = \sqrt{-1}$ and ω is the angular frequency (in radians). The need for CPE comes from the non-ideal impedance response of electrode processes, which, instead of uniform and single valued time constants for each physical phenomenon or reaction, usually show dispersions of time constants that are attributed to surface heterogeneities or to distributions of reactivity or current and potential along the electrode surface [45]. The capacitances were subsequently calculated from the CPEs using the equation proposed by Brug *et al* [46],

$$C = Y_0^{1/n}\left(1/R_1 + 1/R_2\right)^{(n-1)/n}, \qquad (2)$$

where R_1 is the resistance in series and R_2 the resistance in parallel with the CPE.

The evolution of the parameters with the time of immersion is depicted in figure 10. The fit results confirm the higher impedance of sol–gel coated systems but also show a fast decrease of resistance and increase of capacitance of the films applied over nanotubes. After three weeks of immersion in SBF 37 °C, the response of Ti-TNT135-SG is close to the uncoated surfaces and Ti-TNT-65-SG is very close to the Ti-SG. This evolution suggests water uptake from the coating and accumulation in the nanotube-film interface leading to coating delamination. The high R_{PL} and low C_{surf}, C_{PL} and C_{BL} are related to the small area of the pores and defects on the sol–gel films. The values of R_{surf} and R_{BL} are not presented because very high values, close to the numerical fitting limit, were obtained. The measurements ended in a capacitive region and lower frequencies would be needed to accurately detect the resistive response.

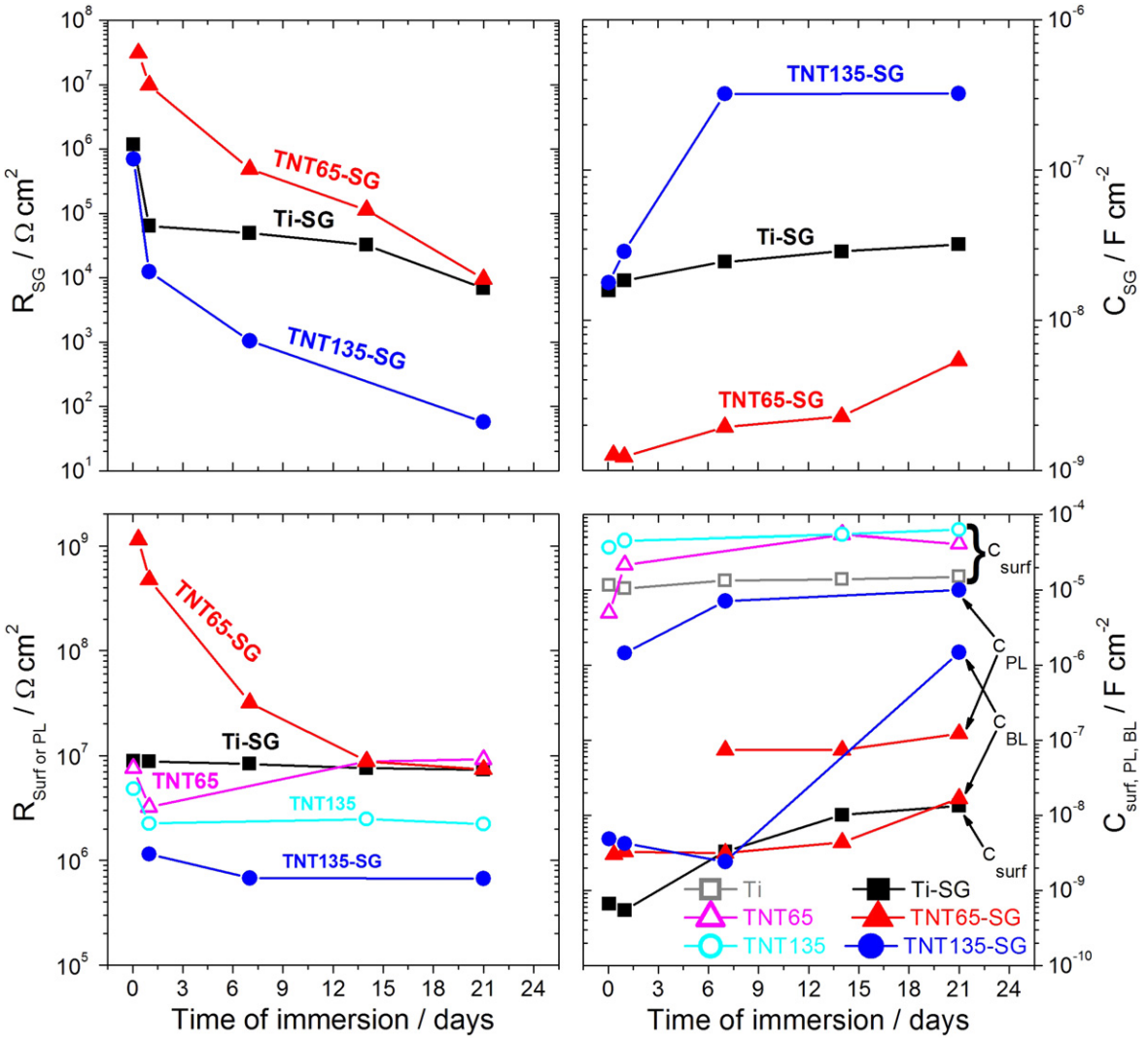

Figure 10. Evolution with time of immersion of the parameters obtained by numerical fitting of the impedance spectra.

The polarization curves showed small currents near OCP in both cathodic and anodic directions which are an indication of the good corrosion resistance of the tested materials. The higher corrosion resistance is related with the presence of the nanotubes and sol–gel film since both represent a barrier to the electrochemical reactions. The impedance values were similar to, and in some cases even higher than, the values reported in the literature for other hybrid organic-inorganic coatings in metallic surfaces [1, 3, 37, 47].

4. Conclusions

We have demonstrated a new strategy for the improvement of the adhesion properties and the corrosion resistance of metallic titanium. Highly ordered TiO_2 nanotubular structures with two different diameters were successfully obtained by anodization of titanium foil. PDMS-TEOS sol–gel films were synthetized and used as coating on TiO_2 nanotubular arrays. Investigations have shown that the combination of titanium nanotubes with the PDMS-TEOS sol–gel coating improves anti-corrosive behavior of metallic titanium. However, with time occurs an increase of the capacitance and a decrease on the resistance of the films, mostly due to water uptake and consequently some rupture of the sol–gel films used. The structure with the smaller diameter of nanotubes (65 nm) and PDMS-TEOS sol–gel film have shown a maximal improvement in the corrosion resistance and the adhesion properties compared to the other samples, having the potential to be used in the production of materials for clinical purposes.

Acknowledgements

This work has been supported by the FEDER funds, through the Program COMPETE, FCT (Fundação para a Ciência e Tecnologia) funds by the grant SFRH/BD/72074/2010 and the Italian Ministry of Education through the project FIRB ‘Rete Nazionale di Ricerca sulle Nanoscienze ItalNanoNet’ (Protocollo: RBPR05JH2P, 2009–2013). We also want to

acknowledge the program which is financing CICECO at present, Pest-C/CTM/LA0011/2011.

References

[1] Gallardo J, Galliano P and Duran A 2001 Bioactive and protective sol–gel coatings on metals for orthopaedic prostheses *J. Sol-Gel Sci. Technol.* **21** 65–74

[2] Hijon N, Manzano M, Salinas A J and Vallet-Regi M 2005 Bioactive CaO-SiO_2-PDMS coatings on Ti6Al4V substrates *Chem. Mater.* **17** 1591–6

[3] Hosseinalipour S M, Ershad-Langroudi A, Hayati A N and Nabizade-Haghighi A M 2010 Characterization of sol–gel coated 316L stainless steel for biomedical applications *Prog. Org. Coat.* **67** 371–4

[4] Yu W-q, Qiu J, Xu L and Zhang F-q 2009 Corrosion behaviors of TiO_2 nanotube layers on titanium in Hank's solution *Biomed. Mater.* **4** 065012

[5] Bolat G, Izquierdo J, Mareci D, Sutiman D and Souto R M 2013 Electrochemical characterization of ZrTi alloys for biomedical applications. Part 2: the effect of thermal oxidation *Electrochim. Acta* **106** 432–9

[6] Garbacz H, Pisarek M and Kurzydlowski K J 2007 Corrosion resistance of nanostructured titanium *Biomol. Eng.* **24** 559–63

[7] Zhao L, Mei S, Chu P K, Zhang Y and Wu Z 2010 The influence of hierarchical hybrid micro/nano-textured titanium surface with titania nanotubes on osteoblast functions *Biomaterials* **31** 5072–82

[8] Zwilling V, Darque-Ceretti E, Boutry-Forveille A, David D, Perrin M Y and Aucouturier M 1999 Structure and physicochemistry of anodic oxide films on titanium and TA6V alloy *Surf. Interface Anal.* **27** 629–37

[9] Paulose M, Varghese O K, Mor G K, Grimes C A and Ong K G 2006 Unprecedented ultra-high hydrogen gas sensitivity in undoped titania nanotubes *Nanotechnology* **17** 398–402

[10] Varghese O K, Paulose M and Grimes C A 2009 Long vertically aligned titania nanotubes on transparent conducting oxide for highly efficient solar cells *Nat. Nanotechnology* **4** 592–7

[11] Lai Y, Zhuang H, Sun L, Chen Z and Lin C 2009 Self-organized TiO_2 nanotubes in mixed organic–inorganic electrolytes and their photoelectrochemical performance *Electrochim. Acta* **54** 6536–42

[12] Galstyan V, Vomiero A, Comini E, Faglia G and Sberveglieri G 2011 TiO_2 nanotubular and nanoporous arrays by electrochemical anodization on different substrates *RSC Adv.* **1** 1038–44

[13] Mor G K, Shankar K, Paulose M, Varghese O K and Grimes C A 2005 Use of highly-ordered TiO_2 nanotube arrays in dye-sensitized solar cells *Nano Lett.* **6** 215–8

[14] Kyerematen N A, Vacandio F, Sougrati M T, Martinez H, Jumas J C, Knauth P and Djenizian T 2013 Effect of Sn-doping on the electrochemical behaviour of TiO_2 nanotubes as potential negative electrode materials for 3D Li-ion micro batteries *J. Power Sources* **224** 269–77

[15] Kyerematen N A, Lebouin C, Knauth P and Djenizian T 2013 The electrochemical behaviour of TiO_2 nanotubes with Co_3O_4 or NiO submicron particles: composite anode materials for Li-ion micro batteries *Electrochim. Acta* **88** 814–20

[16] Galstyan V, Vomiero A, Concina I, Braga A, Brisotto M, Bontempi E, Faglia G and Sberveglieri G 2011 Vertically aligned TiO_2 nanotubes on plastic substrates for flexible solar cells *Small* **7** 2437–42

[17] Mazare A, Paramasivam I, Lee K and Schmuki P 2011 Improved water-splitting behaviour of flame annealed TiO_2 nanotubes *Electrochem. Commun.* **13** 1030–4

[18] Galstyan V, Comini E, Faglia G, Vomiero A, Borgese L, Bontempi E and Sberveglieri G 2012 Fabrication and investigation of gas sensing properties of Nb-doped TiO_2 nanotubular arrays *Nanotechnology* **23** 235706

[19] Yu W-Q, Qiu J and Zhang F-Q 2011 *In vitro* corrosion study of different TiO_2 nanotube layers on titanium in solution with serum proteins *Colloids Surf.* B **84** 400–5

[20] Minagar S, Berndt C C, Wang J, Ivanova E and Wen C 2012 A review of the application of anodization for the fabrication of nanotubes on metal implant surfaces *Acta Biomater.* **8** 2875–88

[21] Jun S H, Lee E J, Yook S W, Kim H E, Kim H W and Koh Y H 2010 A bioactive coating of a silica xerogel/chitosan hybrid on titanium by a room temperature sol–gel process *Acta Biomater.* **6** 302–7

[22] Zheng C Y, Nie F L, Zheng Y F, Cheng Y, Wei S C, Ruan L Q and Valiev R Z 2011 Enhanced corrosion resistance and cellular behavior of ultrafine-grained biomedical NiTi alloy with a novel SrO-$SiO_{(2)}$-$TiO_{(2)}$ sol–gel coating *Appl. Surf. Sci.* **257** 5913–8

[23] Ballarre J, Manjubala I, Schreiner W H, Orellano J C, Fratzl P and Cere S 2010 Improving the osteointegration and bone-implant interface by incorporation of bioactive particles in sol–gel coatings of stainless steel implants *Acta Biomater.* **6** 1601–9

[24] Wang Q, Zhang P-Z, Wei D-B, Wang R-N, Chen X-H and Wang H-Y 2013 Microstructure and corrosion resistance of pure titanium surface modified by double-glow plasma surface alloying *Mater. Des.* **49** 1042–7

[25] Wu K H, Chao C M, Yang C J and Chang T C 2006 Synthesis and characterization of polydimethylsiloxane-cured organically modified silicate hybrid coatings *Polym. Degrad. Stab.* **91** 2917–23

[26] Wang D and Bierwagen G R 2009 Sol-gel coatings on metals for corrosion protection *Prog. Org. Coat.* **64** 327–38

[27] Zhang Y, Zhang X, Ye H, Xiao B, Yan L and Jiang B 2012 A simple route to prepare crack-free thick antireflective silica coatings with improved antireflective stability *Mater. Lett.* **69** 86–8

[28] Makoto T 2009 Crack formation, exfoliation, and ridge formation in 500 °C annealed sol–gel silica coatings on stainless steel SUS304: part I. Microscopic observations and elemental analyses *Ceram. Int.* **35** 1731–46

[29] Tian X, Chen Q, Song L, Wang Y and Li H 2007 Formation of alkali resistant PDMS–TiO_2–SiO_2 hybrid coatings *Mater. Lett.* **61** 4432–4

[30] Yabuta T, Tsuru K, Hayakawa S and Osaka A 2004 Synthesis of blood compatible PDMS-based organic-inorganic hybrid coatings *J. Sol-Gel Sci. Technol.* **31** 273–6

[31] Ibrahim W A W, Ismail W N W, Keyon A S A and Sanagi M M 2011 Preparation and characterization of a new sol–gel hybrid based tetraethoxysilane-polydimethylsiloxane as a stir bar extraction sorbent materials *J. Sol-Gel Sci. Technol.* **58** 602–11

[32] Kokubo T and Takadama H 2006 How useful is SBF in predicting *in vivo* bone bioactivity? *Biomaterials* **27** 2907–15

[33] Zwilling V, Aucouturier M and Darque-Ceretti E 1999 Anodic oxidation of titanium and TA6V alloy in chromic media. An electrochemical approach *Electrochim. Acta* **45** 921–9

[34] Mazzarolo A, Curioni M, Vicenzo A, Skeldon P and Thompson G E 2012 Anodic growth of titanium oxide: electrochemical behaviour and morphological evolution *Electrochim. Acta* **75** 288–95

[35] Huang H-H 2002 Electrochemical impedance spectroscopy study of strained titanium in fluoride media *Electrochim. Acta* **47** 2311–8
[36] Shukla A K and Balasubramaniam R 2006 Effect of surface treatment on electrochemical behavior of CP Ti, Ti–6Al–4V and Ti–13Nb–13Zr alloys in simulated human body fluid *Corros. Sci.* **48** 1696–720
[37] Hang R, Huang X, Tian L, He Z and Tang B 2012 Preparation, characterization, corrosion behavior and bioactivity of Ni_2O_3-doped TiO_2 nanotubes on NiTi alloy *Electrochim. Acta* **70** 382–93
[38] Contu F, Elsener B and Böhni H 2002 Characterization of implant materials in fetal bovine serum and sodium sulfate by electrochemical impedance spectroscopy. I. Mechanically polished samples *J. Biomed. Mater. Res.* **62** 412–21
[39] Saji V S, Choe H C and Brantley W A 2009 An electrochemical study on self-ordered nanoporous and nanotubular oxide on Ti–35Nb–5Ta–7Zr alloy for biomedical applications *Acta Biomater.* **5** 2303–10
[40] Liu C, Wang Y, Wang M, Huang W and Chu P K 2011 Electrochemical stability of TiO_2 nanotubes with different diameters in artificial saliva *Surf. Coat. Technol.* **206** 63–7
[41] Pan J, Thierry D and Leygraf C 1996 Electrochemical impedance spectroscopy study of the passive oxide film on titanium for implant application *Electrochim. Acta* **41** 1143–53
[44] González J E G and Mirza-Rosca J C 1999 Study of the corrosion behavior of titanium and some of its alloys for biomedical and dental implant applications *J. Electroanal. Chem.* **471** 109–15
[43] Assis S L D, Wolynec S and Costa I 2006 Corrosion characterization of titanium alloys by electrochemical techniques *Electrochim. Acta* **51** 1815–9
[44] Figueira N, Silva T M, Carmezim M J and Fernandes J C S 2009 Corrosion behaviour of NiTi alloy *Electrochim. Acta* **54** 921–6
[45] Orazem M E and Tribollet B 2008 *Electrochemical Impedance Spectroscopy* (New York: Wiley) pp 233–63
[46] Brug G J, van den Eeden A L G, Sluyters-Rehbach M and Sluyters J H 1984 The analysis of electrode impedances complicated by the presence of a constant phase element *J. Electroanal. Chem. Interfacial Electrochem.* **176** 275–95
[47] Raps D, Hack T, Wehr J, Zheludkevich M L, Bastos A C, Ferreira M G S and Nuyken O 2009 Electrochemical study of inhibitor-containing organic–inorganic hybrid coatings on AA2024 *Corros. Sci.* **51** 1012–21